Published in final edited form as:
Mol Microbiol. 2013 January ; 87(1): 152–167. doi:10.1111/mmi.12088.

Acetoacetyl-CoA synthetase activity is controlled by a protein acetyltransferase with unique domain organization in *Streptomyces lividans*

Alex C. Tucker[1] and **Jorge C. Escalante-Semerena**[2,*]
[1]Department of Bacteriology, University of Wisconsin
[2]Department of Microbiology, University of Georgia

Summary

GCN5-type*N*-acetyltransferases (GNATs) are enzymes that catalyze the transfer of the acetyl group from acetyl-CoA to a primary amine. GNATs are conserved in all domains of life. Some members of this family of enzymes acetylate the side chain of specific lysine residues in proteins of diverse function. In bacteria, GNAT-catalyzed protein acetylation regulates carbon metabolism, RNA metabolism, and transcriptional regulation. Metabolic regulation in *Streptomyces* species is of interest due to the role of these organisms in natural product synthesis. Here we identify *Sl*PatA, a GNAT in *S. lividans* with unique domain organization, and a new acetylation target, namely acetoacetyl-CoA synthetase (*Sl*AacS). The latter has homologues in all domains of life. *In vitro* and *in vivo* evidence show that *Sl*AacS is a bona fide acetoacetyl-CoA synthetase. *Sl*PatA acetylates *Sl*AacS more efficiently than it does acetyl-CoA synthetase, an enzyme known to be under acetylation control. *Sl*PatA acetylates *Sl*AacS at the active site residue Lys617 and acetylation inactivates *Sl*AacS. Acetylated *Sl*AacS was deacetylated by a sirtuin-type protein deacetylase. *Sl*AacS acetylation/deacetylation may represent a conserved mechanism for regulation of acetoacetyl-CoA synthetase activity in all domains of life.

Introduction

GCN5-related *N*-acetyltransferase (GNAT) enzymes catalyze the transfer of an acetyl moiety from acetyl-coenzyme A (Ac-CoA) to a primary amine of small molecules and proteins. GNATs, named for the homology to the yeast GCN5 protein (yGCN5p), are identified by signature sequence motifs and structurally homology (Shaw *et al.*, 1993). GNATs are conserved in all domains of life, and represent one of the largest proteins super families (Vetting *et al.*, 2005). GNATs are involved in acetylation of antibiotics, hormones, tRNA, histones, metabolic enzymes, and transcription factors, implicating GNATs in a wide variety of cellular processes (Vetting et al., 2005, Thao *et al.*, 2010, Ikeuchi *et al.*, 2008, Thao & Escalante-Semerena, 2011b, Spange *et al.*, 2009). Protein lysine acetylation by GNATs occurs on the epsilon amino group of the lysine side chain. Acetylation neutralizes the positive charge of the lysine side chain altering the side-chain chemistry. Protein acetylation has been documented in all domains of life (Soppa, 2010), but recent proteomic approaches performed in eukaryotes (Kim *et al.*, 2006, Choudhary *et al.*, 2009, Weinert *et al.*, 2011, Zhao *et al.*, 2010) and bacteria (Zhang *et al.*, 2009, Yu *et al.*, 2008, Crosby *et al.*, 2012) have expanded our view of the potential role of this posttranslational modification in

*Correspondence should be sent to: Department of Microbiology, University of Georgia, 527 Biological Sciences Building, 120 Cedar Street, Athens, GA 30602 USA, Tel: 706-542-2651; Fax: 706-542-2815; jcescala@uga.edu.

The authors have no conflict of interest to declare.

cell physiology. As new protein acetylation targets and the concomitant protein acetyltransferases are identified, the role of acetylation on protein and cellular functions is broadened.

GNATs are the only class of protein acetyltransferases identified in bacteria. The Gram-negative γ-proteobacterium *Salmonella enterica* encodes a protein acetyltransferase *Se*Pat that contains a large *N*-terminal domain (~700 residues) with homology to NDP-forming CoA synthetases and a *C*-terminal GNAT domain (~200 residues) (Starai & Escalante-Semerena, 2004). *Se*Pat lacks NDP-forming Ac-CoA synthetase activity, and the role of the domain remains unclear. Biochemical studies indicate that the *N*-terminal domain of *Se*Pat may be required for acetyltransferase activity, subunit interactions, and positive cooperativity (Thao & Escalante-Semerena, 2011a). *Se*Pat uses acetyl-CoA to acetylate acetyl-CoA synthetase (*Se*Acs) and propionyl-CoA to propionylate propionyl-CoA synthetase (PrpE) (Garrity *et al.*, 2007, Takenoya *et al.*, 2010). In each case, acylation occurs at the active site lysine of the CoA synthetase and inactivates the enzyme. Specifically, lysine acylation prevents the first half reaction that activates the fatty acid to the corresponding fatty-acyl-AMP intermediate. In each case, deacylation reactivates the enzyme (Starai *et al.*, 2002, Garrity et al., 2007).

In the photoheterotrophic purple non-sulfur α-proteobacterium *Rhodopseudomonas palustris*, a *Se*Pat homologue (*Rp*Pat), and a single-domain GNAT, *Rp*KatA, regulate organic acid degradation by acetylating and inactivating seven acyl-CoA synthetases and three aryl-CoA synthetases (Crosby *et al.*, 2010, Crosby et al., 2012). Acetylation of the acyl- or aryl- CoA synthetases has the same effect as seen in *S. enterica*. Notably, the protein deacetylation system of *R. palustris* is more complex than the one in *S. enterica*. *R. palustris* encodes a sirtuin-type, NAD^+-dependent deacetylase *Rp*SrtN, and a Zn(II)-dependent histone deacetylase homologue *Rp*LdaA. *Rp*LdaA hydrolyzes the acetyl group from acetyllysine releasing free acetate and reactivating acyl-CoA synthetases. At present, the only protein with acetyllysine deacetylase activity in *S. enterica* is a sirtuin encoded by the *cobB* gene (Tsang & Escalante-Semerena, 1998, Tucker & Escalante-Semerena, 2010). Protein acetyltransferases have also been described in Gram-positive bacteria. *Bacillus subtilis* encodes a single domain GNAT, AcuA, which acetylates acetyl-CoA synthetase (*Bs*AcsA) (Gardner *et al.*, 2006). *Mycobacterium tuberculosis* and *M. smegmatis* encode protein acetyltransferases, *Mt*PatA and *Ms*Pat, respectively, with a cyclic-AMP binding domain fused to the *N*-terminus of a GNAT domain (Nambi *et al.*, 2010). Binding of cAMP to *Mt*PatA activates the enzyme by exposing the catalytic site (Lee *et al.*, 2012). *Ms*Pat acetylates a universal stress protein and Ac-CoA synthetase in *M. smegmatis* (Nambi et al., 2010, Xu *et al.*, 2011).

Recently, Mikulik et al. demonstrated that Ac-CoA synthetase from the actinomycete *Streptomyces coelicolor* is acetylated *in vivo* (Mikulik *et al.*, 2012), but the acetyltransferase responsible for this modification remains unidentified. *S. coelicolor* encodes 77 putative GNAT acetyltransferases (Pfam00583), whilst the genome of the closely related species *S. lividans* (Kawamoto & Ochi, 1998) encodes 72 putative GNATs. However, none of the putative GNATs share end-to-end homology with the known bacterial protein acetyltransferases *Se*Pat, *Ec*Pka, *Rp*Pat, *Rp*KatA, *Bs*AcuA, *Ms*Pat, or *Mt*PatA. Further understanding of the regulation of metabolism in *Streptomyces* species is of interest because of the diversity of natural products synthesized by these organisms (Seow *et al.*, 1997, Courtois *et al.*, 2003, McMahon *et al.*, 2012, Chater, 2006).

Here, we identify a GNAT in *S. lividans* that has protein acetyltransferase activity and contains regions of homology to both the *N*- and *C*-terminal domains of *Se*Pat. The *S. lividans* Pat homologue (*Sl*PatA) can acetylate native Ac-CoA synthetase (*Sl*Acs), albeit to a

limited extent, but acetylates acetoacetyl-CoA synthetase (*Sl*AacS) substantially better. Prior to this work, the regulation of *Sl*AacS activity by lysine acetylation/deacetylation systems was unknown. Consistent with the effect of acetylation on other AMP-forming acyl-CoA synthetases, acetylation of *Sl*AacS inactivated the enzyme, whilst deacetylation reactivated it. We also report evidence that *Sl*PatA acetylates *Sl*AacS *in vivo* in *S. lividans*. Further, we used *E. coli* as a heterologous host to demonstrate *Sl*AacS regulation by *Sl*PatA *in vivo*. In summary, we show that a *Se*Pat homologue with reversed domain organization has bona fide acetyltransferase activity. Our findings raise the possibility that acetoacetyl-CoA synthetase homologues in all domains of life may be also controlled by lysine acetylation/deacetylation systems.

Results

Actinomycetes and the archaeon *Archaeoglobus fulgidus* encode a protein acetyltransferase with unique domain organization

Salmonella enterica and *Rhodopseudomonas palustris* synthesize a protein acetyltransferase Pat enzyme with a large (~700 residues) *N*-terminal domain with homology to NDP-forming CoA synthetases and a C-terminal (~200 residues) GNAT domain (Starai & Escalante-Semerena, 2004, Crosby et al., 2010). The EFD66247 locus of the genome of the actinomycete *Streptomyces lividans* encodes a homologue of the *Se*Pat and *Rp*Pat enzymes in which the GNAT and the NDP-forming CoA synthetase-like domains are reversed (Fig. 1A). We note that the DNA sequence of *S. lividans* open reading frame (ORF) EFD66247 currently available in databases contains two mistakes, which we discovered upon cloning and sequencing EFD66247. Our sequencing data showed two changes, a transition (T1787C) and a deletion (ΔT1788). BLASTp searches performed with the protein encoded by the corrected DNA sequence identified a full-length NDP-forming CoA synthetase-like domain homologous to the ones found in *Se*Pat and *Rp*Pat. Further bioinformatics analysis of the corrected sequence of ORF EFD66247 revealed that such reverse domain organization of the putative protein was also present in homologues presumably synthesized by other actinomycetes and the archaeon *Archaeoglobus fulgidus*. The predicted primary sequence of the EFD66247 protein contained a proline-rich sequence (P663-P753, 26.4% proline) that included a degenerate G-P-S motif (Fig. 1B) (Beck & Brodsky, 1998).

The EFD66247 protein (hereafter *Sl*PatA) *is* a functional protein acetyltransferase

*Se*Pat and *Rp*Pat have been shown to acetylate the acetyl-CoA synthetase (Acs) enzymes from *S. enterica* and *R. palustris*, respectively (Starai & Escalante-Semerena, 2004, Crosby et al., 2010). *Se*Pat and *Rp*Pat acetylate the epsilon amino group of an active-site lysyl side chain, with the concomitant inactivation of the adenylylation activity of Acs (Crosby et al., 2010, Starai & Escalante-Semerena, 2004). Mikulik et al. recently reported that the Acs homologue from *Streptomyces ceolicolor* (*Sc*Acs) was acetylated *in vivo* (Mikulik et al., 2012), suggesting that a protein acetyltransferase was responsible for acetylating Acs in this *Streptomyces* species. We asked whether recombinant *Sl*PatA could acetylate *Sl*Acs *in vitro*. For this purpose, *Sl*PatA was purified to homogeneity and incubated with purified *Sl*Acs (encoded by *S. lividans* locus EFD68454) in the presence of [1-^{14}C]-Ac-CoA. As shown in figure 2A, *Sl*PatA acetylated *Sl*Acs, indicating that *Sl*PatA was a bona fide protein lysine acetyltransferase. To verify the site of acetylation, a *Sl*Acs^{K610A} variant was isolated and tested as a substrate of *Sl*PatA. *Sl*PatA did not modify *Sl*Acs^{K610A}, indicating that the active-site residue K610 was the only site modified by *Sl*PatA. For reference, *Sl*PatA was incubated with *Se*Acs, a known substrate of *Se*Pat (Starai & Escalante-Semerena, 2004), and the active site lysine variant *Se*Acs^{K609A}. *Sl*PatA modified *Se*Acs but not *Se*Acs^{K609A} indicating that *Sl*PatA acetylates only the active-site residue K609 of *Se*Acs. Relative

acetylation of *Sl*Acs and *Se*Acs was quantified using digital light units. *Sl*PatA modified *Se*Acs approximately 30-fold more efficiently than *Sl*Acs.

To compare the effect of *Sl*PatA-mediated acetylation on *Sl*Acs and *Se*Acs activity, *Sl*Acs or *Se*Acs was incubated with *Sl*PatA in the presence or absence of acetyl-CoA. When *Sl*Acs was incubated with *Sl*PatA in the presence of Ac-CoA, *Sl*Acs retained approximately 75% of its activity relative to the no acetyl-CoA control (Fig. 2B). This result suggested that *Sl*PatA acetylation of *Sl*Acs was inefficient. *Sl*PatA inactivated *Se*Acs within 90 minutes of incubation with Ac-CoA, confirming that *Se*Acs was a better substrate for *Sl*PatA than *Sl*Acs under the conditions tested. Additionally, these data confirm that *Sl*PatA acted catalytically. As a point of reference, under the conditions used *Se*Pat fully inactivated *Se*Acs (Starai & Escalante-Semerena, 2004).

*Sl*PatA acetylates an acetoacetyl-CoA synthetase homologue from *S. lividans*

Because *Sl*PatA acetylation of *Sl*Acs was inefficient, we looked for additional *Sl*PatA substrates in *S. lividans*. *Se*Pat homologues have been shown to acylate members of the AMP-forming acyl-CoA synthetase family of enzymes (Starai & Escalante-Semerena, 2004, Garrity et al., 2007, Crosby et al., 2012, Crosby et al., 2010). The closest homologue of *Sl*Acs we found in *S. lividans* was a putative acetoacetyl-CoA synthetase (hereafter *Sl*AacS, encoded by locus EFD70521), whose primary sequence was 39% identical to that of the acetoacetyl-CoA synthetase from rat liver (Ito *et al.*, 1984). *Sl*AacS homologues contained the catalytic residue Lys617 (Table 1), which raised the possibility that *Sl*AacS could be acetylated. To test this possibility, *Sl*PatA and *Sl*AacS were incubated in the presence of [1-^{14}C]-Ac-CoA. As shown in figure 3, *Sl*PatA efficiently used [1-^{14}C]-Ac-CoA to modify *Sl*AacS, and residue K617 was the only site of acetylation in *Sl*AacS. Under the same assay conditions, *Sl*PatA acetylated 15-fold more *Sl*AacS than *Sl*Acs, indicating that *Sl*AacS was a substantially better substrate than *Sl*Acs for *Sl*PatA.

*Sl*AacS is a functional acetoacetyl-CoA synthetase *in vivo*

We used strains of *Escherichia coli* to assess *in vivo* the ability of *Sl*AacS to convert acetoacetate to acetoacetyl-CoA (Fig. 4A). *E. coli* encodes a protein acetyltransferase (Pka) homologous to *Se*Pat and sirtuin-type protein deacetylase (CobB). Growth experiments were done in a Δ*pka* Δ*cobB E. coli* strain background to avoid potential *Sl*AacS modification by the *E. coli* acetylation machinery. *E. coli* grows on acetoacetate by first converting it to acetoacetyl-CoA using the acetyl-CoA:acetotacetate CoA transferase enzyme (AtoDA, EC 2.8.3.8). In the second step of the pathway, the 3-ketoacyl-CoA thiolase (AtoB, EC 2.3.1.16) enzyme converts acetoacetyl-CoA and CoA to two molecules of acetyl-CoA, which enter central metabolism (Fig. 4A) (Pauli & Overath, 1972). *E. coli* encodes a second 3-ketoacyl-CoA thiolase, FadA, with a substrate preference for mid-length chain fatty acids that is capable of using acetoacetate as a substrate to generate two molecules of Ac-CoA (Staack *et al.*, 1978). An *E. coli atoDA* strain cannot grow on acetoacetate because it cannot convert acetoacetate to acetoacetyl-CoA (Pauli & Overath, 1972). An *E. coli atoB fadA* strain cannot grow on acetoacetate due to the lack of acetoacetyl-CoA thiolase activity (Jenkins & Nunn, 1987). As shown in figure 4B, when *Sl*AacS encoded by the native *S. lividans aacS* allele was ectopically produced in *E. coli*, growth of the Δ*atoDA* Δ*cobB* Δ*pka* strain on acetoacetate was restored. The final culture density was comparable to that reached when wild type alleles of *atoDA* were provided in *trans*. These data suggest that *Sl*AacS converted acetoacetate to acetoacetyl-CoA compensating for the absence of AtoDA in the *atoDA* strain. The difference in the growth rate of the strain complemented with native *S. lividans aacS* alleles may be due to codon bias of the *S. lividans* allele, differences in enzyme kinetic parameters, or enzyme stability in *E. coli* at 37°C.

To determine the substrate specificity for *Sl*AacS, the AMP-forming CoA synthetase activity of *Sl*AacS was measured using a continuous spectrophotometric assay with CoA, ATP, and organic acids structurally similar to, and including, acetoacetate (see *Experimental procedures* for all substrates tested). *Sl*AacS efficiently activated acetoacetate to acetoacetyl-CoA [12 ± 2 μmol AMP min^{-1} mg^{-1}) and β-hydroxybutyrate to β-hydroxybutyryl-CoA (2 ± 0.2 μmol AMP min^{-1} mg^{-1}). *Sl*AacS specific activities for all other compounds tested were <0.1 μmol AMP min^{-1} mg^{-1}. Clearly, acetoacetate was the preferred substrate of *Sl*AacS, indicating that *Sl*AacS was an acetoacetyl-CoA synthetase (EC 6.2.1.16). To confirm the identity of the AacS reaction product, the substrates ATP, CoA, and acetoacetate were incubated in the presence or absence of *Sl*AacS. High performance liquid chromatography (HPLC) was used to separate products from reagents. The enzyme-containing reaction produced a single unique peak with a retention time of 7.25 min. Mass spectral analysis (positive mode) of this sample revealed a molecular ion with a *m/z* of 852.3, corresponding to the expected mass of acetoacetyl-CoA (851.6 amu).

Lys617 is critical for *Sl*AacS activity and acetylation of Lys617 inactivates *Sl*AacS

In *Sl*AacS, Lys617 is a conserved active site residue, and the site acetylated by *Sl*PatA (Fig. 3A). To assess the role of Lys617 in *SlAacS* activity, site-directed mutagenesis was used to generate *aacS* alleles encoding *Sl*AacS^{K617A} and *Sl*AacS^{K617Q} variants. Alanine served as a catalytically inert substitution and glutamine served as a structural mimic for acetyl-lysine. Relative to the activity of wild-type *Sl*AacS (9.6 ± 0.4 μmol AMP min^{-1} mg^{-1}), both *Sl*AacS^{K617A} and *Sl*AacS^{K617Q} variants were ~20-fold less active (<0.5 μmol AMP min^{-1} mg^{-1}) indicating that Lys617 was critical for activity, lending support to the hypothesis that acetylation of Lys617 inactivated the enzyme.

To test the effect of *Sl*AacS Lys617 acetylation directly, *Sl*AacS was incubated with *Sl*PatA in the presence or absence of acetyl-CoA. In the presence of both acetyl-CoA and *Sl*PatA, *Sl*AacS activity was reduced >97% indicating that *Sl*PatA acetylation of Lys617 effectively decreases *Sl*AacS activity (Fig. 5).

*Sl*AacS is deacetylated and reactivated by sirtuin deacetylase

Acetylation of CoA-ligases is reversed by deacetylases (Starai et al., 2002, Garrity et al., 2007, Crosby et al., 2010, Crosby et al., 2012). The *S. lividans* genome encodes three putative deacetylases, namely two NAD^+-dependent sirtuin-type protein deacetylases [EFD65580 (*Sc*CobB2), EFD71509 (*Sc*CobB1)], and one homologue of the *R. palustris* zinc-dependent protein deacetylase *Rp*LdaA (EFD68590). In *S. coelicolor*, *Sc*CobB1 (100% identity to EFD71509) deacetylates *Sc*Acs *in vitro* (Mikulik et al., 2012). For unknown reasons, our attempts to purify or enrich for active *S. lividans* deacetylases in *E. coli* extracts were unsuccessful. To circumvent this problem, we used the *Salmonella enterica* CobB (*Se*CobB) sirtuin deacetylase enzyme (Starai et al., 2002, Tucker & Escalante-Semerena, 2010), which has been shown to deacetylate heterologous acyl- and aryl-CoA synthetases (Crosby et al., 2010). We used the short form of *Se*CobB (SeCobB$_S$) sirtuin (Tucker & Escalante-Semerena, 2010) to demonstrate the reversibility of the acetylation of *Sl*AacS Lys617. *Sl*AacS was acetylated with *Sl*PatA and [^{14}C-1]-Ac-CoA, followed by incubation with *Se*CobB$_S$ in the absence and presence of NAD^+. In the presence of *Se*CobB$_S$ and NAD^+, the amount of radioactivity associated with *Sl*AacS decreased below the limit of detection indicating that *Se*CobB$_S$ deacetylated *Sl*AacS (Fig. 6A), demonstrating that *Sl*AacS acetylation was reversible.

We assessed whether deacetylation of *Sl*AacS^{Ac} by *Se*CobB$_s$ would restore *Sl*AacS activity. To do this, we incubated *Sl*PatA with *Sl*AacS and acetyl-CoA. After incubation, buffer was exchanged to remove excess acetyl-CoA. *Se*CobB$_s$ and NAD^+ were added to the reaction

mixture prior to a second incubation period, after which *Sl*AacS activity was restored to levels comparable to the unacetylated *Sl*AacS control (Fig. 6B). Specific activity of unacetylated *Sl*AacS was reduced when compared to the specific activity measurements reported for the substrate specificity determination. This discrepancy was likely due to instability of the enzyme during the acetylation reaction, buffer exchange, and deacetylation reaction.

*Sl*AacS is acetylated *in vivo* during growth of *S. lividans* in the presence of acetoacetate

We assessed whether or not *Sl*AacS was acetylated *in vivo* in *S. lividans* and whether *Sl*PatA catalyzed the modification of *Sl*AacS. H_6-*Sl*AacS was purified from *S. lividans patA*$^+$ and Δ*patA* strains grown in minimal medium supplemented with acetoacetate. We then assessed the acetylation state of *Sl*AacS by two methods. First, we isolated H_6-*Sl*AacS enzymes from each strain and determined whether or not they were acetylated. To do this, we used Western blot analysis with polyclonal anti-acetyllysine antibodies. Results of control experiments with non-acetylated and *in-vitro* acetylated *Sl*AacS (Fig. 7A) showed that acetyllysine was readily detected under the conditions used. A strong signal was detected for acetyllysine in *Sl*AacS isolated from *S. lividans patA*$^+$, whilst the level of acetyllysine in *Sl*AacS isolated from the *S. lividans* Δ*patA* strain was not significantly above background (Fig. 7A). Based on these data we inferred that *Sl*AacS was acetylated *in vivo* and that *Sl*PatA was the only protein acetyltransferase that modified *Sl*AacS under the conditions tested. To confirm the modification of *Sl*AacS, H_6-*Sl*AacS isolated from *S. lividans patA*$^+$ was subjected to trypsin digestion and the resulting peptides were analyzed by LC/MS/MS. Sequence determination of the peptides identified K617 as the single site of acetylation of *Sl*AacS (Figure S1).

Secondly, we quantified the fraction of acetylated *Sl*AacS present in the cell under growth the conditions used. To do this, we isolated H_6-*Sl*AacS proteins from *S. lividans patA*$^+$ and *S. lividans* δ*patA* strains and incubated them with *Se*CobB and NAD^+ *in vitro*. The premise here was that the activity of acetylated H_6-*Sl*AacS should increase upon deacetylation by *Se*CobB, whilst the activity of non-acetylated H_6-*Sl*AacS should remain unchanged after incubation with *Se*CobB and NAD^+. In the presence of the co-substrate NAD^+, *Se*CobB deacetylated H_6-*Sl*AacS isolated from the *S. lividans patA*$^+$ strain, resulting in a 2.5-fold increase in H_6-*Sl*AacS activity (Figure 7B). In contrast, incubation of H_6-*Sl*AacS isolated from the *S. lividans* Δ*patA* strain with *Se*CobB and NAD^+ did not change the activity of H_6-*Sl*AacS (data not shown). Collectively, these data indicated that, in *S. lividans*, *Sl*PatA modulated the activity of H_6-*Sl*AacS *in vivo*.

*Sl*AacS is required for growth of *S. lividans* on acetoacetate

As shown above, *Sl*AacS was acetylated in *S. lividans* during growth in minimal medium supplemented with acetoacetate. On the basis of these results we made several predictions. First, we posited that *S. lividans* would not grow if putative genes encoding known protein deacetylases were deleted from the chromosome. This idea assumed that the absence of deacetylase activity would not affect in any way the ability of *Sl*PatA to acetylate *Sl*AacS resulting in a net accumulation of acetylated, inactive *Sl*AacS and should not support growth on acetoacetate. To test this hypothesis, we constructed a strain carrying chromosomal deletions of all three genes encoding putative protein deacetylases, i.e., ΔEFD68590 (Zn(II)-dependent deacetylase), ΔEFD65580 (*Sl*CobB2 sirtuin), and ΔEFD71509 (*Sl*CobB1 sirtuin). Surprisingly, growth of the ΔEFD68590 ΔEFD65580 ΔEFD71509 (JE16752) strain was comparable to that of wild-type *S. lividans* on acetoacetate (Fig. 8).

To assess whether or not *Sl*AacS was required for growth of *S. lividans* on acetoacetate, we constructed a *S. lividans* Δ*aacS* strain. Strains were tested for their ability to grow on

minimal medium supplemented with acetoacetate. Unlike the wild-type strain, the Δ*aacS* (JE16758) strain grew poorly on acetoacetate (Fig. 8), indicating that *Sl*AacS activity was required for growth of *S. lividans* on this carbon and energy source.

In vivo acetylation control of *Sl*AacS activity in a heterologous system

We used *E. coli* to demonstrate that *Sl*PatA activity controlled *Sl*AacS function *in vivo*. The *E. coli pka* allele, encoding a *Se*Pat protein acetyltransferase homologue, was disrupted to avoid potential modification of *Sl*AacS by the *E. coli* protein acetylation machinery. As shown in figure 4B, an *atoDA pka* strain of *E. coli* can use *Sl*AacS to activate acetoacetate for subsequent use as a source of carbon and energy. Based on these data we predicted that, although *Sl*PatA would inactivate *Sl*AacS in *E. coli*, such negative effect on *Sl*AacS activity would be balanced by the activity of the *E. coli* CobB sirtuin deacetylase enzyme (*Ec*CobB, 92% identical to *Se*CobB). This prediction is illustrated in figure 9A. For this purpose, the coding sequence of the *S. lividans aacS* allele was optimized for expression in *E. coli*. We hypothesized that in the absence of *Ec*CobB, the Δ*atoDA* Δ*cobB* Δ*pka* / p*aacS*$^{+}$ p*patA*$^{+}$ strain (JE16969, the letter `p' preceding a gene denotes that it is plasmid-borne) would not grow on acetoacetate due to the accumulation of inactive *Sl*AacS^{Ac}, a prediction that was experimentally confirmed, as shown in figure 9B (solid circles). These data showed that *Sl*PatA acetylation of *Sl*AacS modulated *Sl*AacS activity *in vivo* in a heterologous host. Synthesis of *Sl*PatA in an *E. coli cobB*$^{+}$ strain did not have a deleterious effect during growth on acetoacetate (Fig. 9B, open circles), indicating reversibility of *Sl*AacS acetylation by *Ec*CobB sirtuin deacetylation *in vivo*. Results of control experiments demonstrated that *cobB* was not required for growth of *E. coli* Δ*atoDA* Δ*pka* / p*aacS*$^{+}$ in the absence of *Sl*PatA (p*patA*$^{+}$, data not shown).

Discussion

A new GNAT and a new acyl-CoA synthetase in *S. lividans* reveal a functional lysine acetylation system that may control acetoacetate metabolism in this and other actinomycetes

This work identified two new functions in *S. lividans.* One is a previously uncharacterized GNAT-type protein acetyltransferase with unique domain organization. This GNAT is conserved in some actinomycetes and in the archaeon *Archaeoglobus fulgidus* (Fig. 1). The existence of this new GNAT (encoded by EFD66247) was revealed through bioinformatics analysis and DNA sequencing to correct database mistakes in the sequence of the gene. The above mentioned analysis showed a reversal in the domain organization of the protein (Fig. 1) with homology to other protein acetyltransferase (Pat) enzymes previously described. Hence we propose the name *Sl*PatA. The second new function is an acyl-CoA synthetase (encoded by EFD70521) responsible for the activation of acetoacetate to acetoacetyl-CoA, thus we propose the name *Sl*AacS for this protein. The name and functional assignments of these proteins are experimentally supported by *in vivo* and *in vitro* data (Figs. 3, 4, 5, 8). Collectively, the data show that *Sl*AacS is used by *S. lividans* to grow on acetoacetate, and that *Sl*PatA catalyzes the acetyl-CoA-dependent acetylation of *Sl*AacS.

The reversal of the domain organization of *Sl*PatA does not affect its acetyltransferase function

In *Sl*PatA, the large *C*-terminal domain (NDP-forming CoA ligase homologue) is found at the *N*-terminus of its homologues in *S. enterica*, *E. coli*, and *R. palustris*. This type of domain inversion has been observed in NDP-forming CoA ligases (Sánchez *et al.*, 2000) and phosphoenolpyruvate-dependent sugar:phosphotransferase systems (Reizer & Saier, 1997). This report expands the phenomenon of domain order reversal to Pat-type GNATs. Further

characterization of these multi-domain GNAT enzymes is necessary to understand the how the activity of these enzymes may be regulated.

The role of the large NDP-forming CoA ligase-like domain in *Sl*PatA homologues remains unknown. Recently reported data obtained with *Se*Pat suggest that this large domain may be responsible multimerization (Thao & Escalante-Semerena, 2011a). Such information is not yet available for *Sl*Pat. The domain inversion in *Sl*PatA may reflect an alternative regulatory mechanism.

The *Sl*PatA *C*-terminal domain contains a proline-rich region with a degenerate G-P-S motif, a signature of the fibrous protein collagen (Hulmes, 1992). In collagen and bacterial proteins with a G-X-Y motif, these motifs adopt extended fibrillar stretches of amino acids (Hulmes, 1992, Xu *et al.*, 2002). In *Klebsiella pneumoniae* strain FG9 a G-X-Y motif stabilizes homotrimers of the polysaccharide de-branching enzyme pullulanase (Charalambous *et al.*, 1988). The role of the proline-rich region of *Sl*PatA in enzyme structure, oligomerization, and activity remains under investigation.

Control of *Sl*AacS activity by *Sl*PatA retains features observed in the control of other acyl-CoA synthetases by lysine acetylation

The mechanism of *Sl*AacS control by acetylation shares several features with previously reported enzymes under the same control. These features are: i) the acetylation site is a conserved lysine residue in the active site (in *Sl*AacS it is Lys617, Table 1); ii) activity of the enzyme is abolished upon acetylation; and iii) the modification can be enzymatically removed by a bona fide sirtuin deacetylase (Fig. 6). At the moment, what is unclear is which deacetylase in *S. lividans* is responsible for activation of *Sl*AacS^{Ac}. Our data (Fig. 8) cannot unambiguously identify the protein deacetylase, if any, that reactivates acetylated *Sl*AacS in *S. lividans*. Further analysis is needed to identify the *Sl*PatA cognate deacetylase.

Pat homologues *Rp*Pat and *Se*Pat (Fig. 1) were previously shown to acetylate and inactivate the acetyl-CoA synthetases *Rp*Acs and *Se*Acs, respectively. Notably, *Sl*PatA acetylates *Sl*AacS more efficiently than it does *S. lividans* acetyl-CoA synthetase, *Sl*Acs (Fig. 2, 5). Mikulik *et al.* demonstrated that Acs from the closely related *S. coelicolor* is acetylated *in vivo* (Mikulik et al., 2012), raising the question of which acetyltransferase acetylates *Sl*Acs in *S. lividans*. Work is currently underway to identify the role of *Sl*PatA and other protein acetyltransferases in *Sl*Acs regulation in *S. lividans*.

Physiological roles of acetoacetyl-CoA synthetase acetylation in bacteria, archaea, and eukaryotes

Clearly, *S. lividans* requires AacS activity for growth on acetoacetate (Fig. 8), however, it is not so clear whether this enzyme is needed to activate internally generated or externally transported acetoacetate. The chemical instability of acetoacetate (Hay & Bond, 1967) makes it likely that the source of substrate for *Sl*AacS is internal.

The *S. lividans* genome encodes five homologues of *E. coli* AtoB, the 3-ketoacyl-CoA thiolase that converts acetoacetyl-CoA and free coenzyme A to two molecules of acetyl-CoA (Fig. 4A), which are likely catabolized via the ethylmalonyl-CoA pathway for the degradation of acetate (Erb *et al.*, 2007), since *S. lividans* lacks the glyoxylate cycle for C_2 compound assimilation (Lewis *et al.*, 2010). Since the conversion of acetoacetate to acetyl-CoA by *Sl*AacS requires input of ATP, we propose that acetylation and inactivation of *Sl*AacS prevents excess ATP and CoA consumption for synthesis of acetyl-CoA. This effect has been demonstrated in *S. enterica* when overproduction of acetyl-CoA synthetase (*Se*Acs) inhibits growth of *S. enterica* on acetate due to ATP depletion and loss of energy charge (Chan *et al.*, 2011).

Cells of all domains of life synthesize acetoacetyl-CoA synthetase, including archaea, bacteria, nematodes, and mammals (Table 1). In the Gram-negative, nitrogen-fixing bacterium *Sinorhizobium meliloti*, the *aacS* homologue *acsA* is required for growth on poly-3-hydroxybutyrate (PHB) cycle intermediates acetoacetate and 3-hydroxybutyrate (Cai *et al.*, 2000). Some bacteria use the PHB cycle to accumulate and store carbon in a reduced form. PHB can then be used as a carbon an energy source during times of physiological stress (Anderson & Dawes, 1990). Acetylation of AacS may regulate the PHB degradation in *S. meliloti* and other organisms that utilize AacS as a step of the PHB cycle, potentially expanding the role of lysine acetylation in prokaryotic cell physiology. The presence of a homologue of *Sl*Pat in *Archaeoglobus fulgidus* raises intriguing questions regarding the physiological role of lysine acylation in this extremely thermophilic, sulfate-reducing archaeon, especially because we did not find *Sl*Pat homologues in any other archaeal genomes in the databases.

In *Caenorhabditis elegans*, the *Sl*AacS homologue SUR-5 negatively regulates a vulval differentiation pathway (Gu *et al.*, 1998). In mammals, acetoacetate-CoA synthetase is important for activation of ketone bodies for cholesterol and fatty acid biosynthesis (Buckley & Williamson, 1973, Geelen *et al.*, 1983). AACS mRNA expression is regulated differentially in adipose tissue of genetically obese and nutritionally obese mice, suggesting that AACS may be important in lipogenesis and ketone body levels during hyper nutritional conditions (Yamasaki *et al.*, 2007).

AacS homologues contain the conserved active site lysine (Table 1). Hence, acetylation of acetoacetyl-CoA synthetase may represent a conserved mechanism of acetoacetyl-CoA synthetase control in these organisms.

Apparent complexity of protein deacetylation in *S. lividans*

The efficient deacetylation of acetylated *Sl*AacS by a sirtuin deacetylase shows that the posttranslational modification of Lys617 is reversible (Fig. 6). The inability of purified *S. lividans* sirtuin-type deacetylase homologues, CobB1 and CobB2, or the zinc-dependent protein deacetylase homolog EFD68590 to deacetylate *Sl*AacS *in vitro* was unexpected because sirtuins from *S. enterica* and *E. coli* deacetylated *Sl*AacS *in vitro* and *in vivo*, respectively (Fig. 6A, 9B). The identity of the enzyme responsible for *Sl*AacS deacetylation *in vivo* remains unclear. *Frankia* sp. CcI3, a related actinomycete, encodes an *Sl*PatA homologue that clusters with an *Sl*AacS homologue and an EFD68590 (Zn(II)-dependent deacetylase) homologue (Fig. S2). This gene clustering suggests that Zn(II)-dependent protein deacetylase EFD68590 may regulate of *Sl*AacS activity.

A triple mutant of the *S. lividans* protein deacetylase homologues grew on acetoacetate (Fig. 8). This result was unexpected because of the accumulation of acetylated *Sl*AacS (Fig. 7A). We propose that: (i) the level of non-acetylated *Sl*AacS in *S. lividans* supports growth on acetoacetate as a carbon source, and deacetylation would not be necessary for growth under these conditions; (ii) not all the *Sl*AacS in the cell is acetylated, and what remains provides sufficient activity to support growth of *S. lividans* on acetoacetate; or (iii) *S. lividans* may encode an additional class of protein deacetylase capable of reactivating *Sl*AacS.

Experimental procedures

Bacterial strains and growth conditions

All strains and plasmids used in this study are listed in Tables S1 and S2, respectively. *Streptomyces* strains are derivatives of *Streptomyces lividans* TK24. ISP-2 medium (Shirling & Gottlieb, 1966) or R2YE medium (Kieser *et al.*, 2000c) was used to culture *S. lividans* on solid medium. Liquid cultures of *S. lividans* were grown in either yeast extract-

malt extract (YEME) rich medium or NMMP medium supplemented with lithium acetoacetate (10 mM) (Kieser et al., 2000c). *S. lividans* liquid cultures were grown in baffled flasks (YEME) or with marine-grade stainless steel springs (NMMP) to aid in cell dispersion. Strains were cultured 3 to 5 days at 30°C or 42°C. When necessary, antibiotics were used at the following concentrations: apramycin, 50 μg ml^{-1} (YEME, ISP-2); thiostrepton, 10 μg ml^{-1} (YEME), 5 μg ml^{-1} (ISP2, R2YE, NMMP).

Unless noted otherwise, all *E. coli* strains used were derivatives of *E. coli* MG1655. *E. coli* strains were grown at 37°C in lysogeny broth (LB, Difco) (Bertani, 1951) or no-carbon essential (NCE) minimal medium (Berkowitz *et al.*, 1968) supplemented with lithium acetoacetate (30 mM), $MgSO_4$ (1 mM), and ampicillin (100 μg ml^{-1}). When necessary, antibiotics were used at the following concentrations: ampicillin, 100 μg ml^{-1}; apramycin, 50 μg ml^{-1}; chloramphenicol, 12.5 μg ml^{-1}. L-(+)-arabinose was added at a final concentration of 50 μM to induce the expression of the *E. coli* codon-optimized *S. lividans aacS* (EFD70521) from the P_{araBAD} promoter. Isopropyl β-D-1-thiogalactopyranoside (IPTG) was added to a final concentration of 50 μM IPTG to induce expression of *S. lividans patA* (EFD66247).

Molecular techniques

DNA manipulations were performed using standard techniques (Elion *et al.*, 2007). Restriction endonucleases were purchased from Fermentas. DNA was amplified using Pfu Ultra II Fusion DNA polymerase (Agilent) or Herculase II Fusion DNA polymerase (Agilent). Site-directed mutagenesis was performed using the Quikchange™ Site Directed Mutagenesis kit (Agilent). Plasmids were isolated using the Wizard Plus SV Miniprep kit (Promega) and PCR products were purified using the Wizard SV Gel and PCR Clean-Up System (Promega). DNA sequencing was performed using BigDye® (ABI PRISM) protocols, and sequencing reactions were resolved at the University of Wisconsin-Madison Biotechnology Center. Oligonucleotide primer sequences are listed in Table S2.

Plasmids used for protein overproduction

The *S. lividans patA* (EFD66247), *aacS* (EFD70521), and *acs* (EFD68454) genes were amplified from purified *S. lividans* TK24 genomic DNA with the primers listed in Table S2. The first codon of *Sl*Acs (GTG) and *Sl*PatA (TTG) were changed to the more common ATG start codon. The DNA fragments were digested with NheI and EcoRI and ligated into pTEV5 (Rocco *et al.*, 2008) cut with the same enzymes. The resulting plasmids p*Sl*PatA1 and p*Sl*AacS1, and p*Sl*Acs1 direct synthesis of *Sl*PatA, *Sl*AacS, and *Sl*Acs, respectively, with *N*-terminal H_6 tags cleavable by recombinant tobacco etch virus (rTEV) protease prepared as described (Blommel & Fox, 2007). Plasmids directing synthesis of $SlAacS^{K617A}$ and $SlAcs^{K610A}$ variants were generated from the p*Sl*AacS1 and p*Sl*Acs1 plasmids using site-directed mutagenesis.

Construction of other plasmids

***E. coli* complementation plasmids—**The *S. lividans aacS* (EFD70521) was amplified from purified *S. lividans* TK24 genomic DNA or from the *aacS* allele whose codon usage was optimized for *E. coli* (Genscript) with the primers that included an optimized ribosome-binding site (Table S2). The native *S. lividans aacS* DNA fragment was cut with HindIII and EcoRI and ligated into pBAD30, cut with the same enzymes. The *E. coli* codon-optimized *S. lividans aacS* DNA fragment was cut with EcoRI and KpnI and ligated into pBAD30 (Guzman *et al.*, 1995) cut with the same enzymes. The resulting plasmids p*Sl*AacS4 and p*Sl*AacS6 express the native *aacS* or optimized *aacS* genes under the control of the arabinose-inducible P_{araBAD}.

S. lividans patA (EFD66247), was amplified from purified *S. lividans* TK24 genomic DNA with the primers listed in Table S2. The *patA* DNA fragment was digested with NdeI and KpnII and ligated into pSRK-Km (Khan *et al.*, 2008) cut with the same enzymes. The resulting plasmid p*Sl*PatA9 express the *S. lividans patA* gene under the control of the $lacI^q$-*lac* promoter-operator system.

***S. lividans* H_6-SlAacS plasmid—**The *S. lividans aacS* gene (EFD70521) was amplified from purified *S. lividans* TK24 genomic DNA with the primers listed in Table S2. The *S. lividans aacS* DNA fragment was cut with XbaI and HindIII and ligated into pSE34 (Ward *et al.*, 1986) cut with the same enzymes. The resulting plasmids p*Sl*AacS5 expresses *S. lividans aacS* with an *N*-terminal H_6 tag under the control of the *erm* promoter.

Construction of gene deletion in *E. coli*

An in-frame deletion of *atoDA* genes in *E. coli* was constructed as using the phage lambda Red recombinase system as previously described (Datsenko & Wanner, 2000).

Construction of gene deletions in *S. lividans*

An in-frame deletion of *S. lividans patA* (EFD66247) was generated using described protocols (Martinez *et al.*, 2004). DNA fragments of 1.5 kb in length were amplified from the DNA upstream and downstream of *S. lividans patA* using purified *S. lividans* TK24 genomic DNA. The resulting fragments were cloned into pKC1139 (Bierman *et al.*, 1992) using the In-Fusion ND Cloning Kit (Clontech) and transformed into *E. coli* Stellar competent cells (Clontech). The resulting plasmid (pKC1139-Δ*patA*) was conjugated into *S. lividans* using the helper strain HB101 harboring pRK2013 (Figurski & Helinski, 1979) on mannitol soya (MS) agar as previously described (Kieser *et al.*, 2000b). Plates were flooded with apramycin (50 $\mu g\ ml^{-1}$ final concentration) 16 h after plating the conjugation mixtures to select for *S. lividans* carrying pKC1130-Δ*patA*. Apramycin-resistant strains were inoculated into 25 ml YEME + apramycin medium and grown in baffled flasks at 30°C for 4 days. Strains were then plated on ISP-2 + apramycin and incubated at 42°C for 3 days to select for a strain in which the plasmid had integrated into the chromosome. Apramycin-resistant strains that grew at 42°C were inoculated into 25 ml YEME in baffled flasks and incubated at 30°C for 4 days and subsequently plated on ISP-2 at 30°C to promote loss of the integrated plasmid. Isolated colonies were screened on ISP-2 for apramycin resistance. Apramycin-sensitive strains were screened by PCR for deletion of the *patA* gene.

Protein purification

***Sl*PatA purification—**Plasmid p*Sl*PatA1 was transformed into *E. coli* strain C41λ(DE3)/pLysSRARE2 (EMD Millipore). The resulting strains were grown overnight and sub-cultured 1:100 (v/v) into 8 liters of superbroth containing ampicillin (100 $\mu g\ ml^{-1}$) and chloramphenicol (12.5 $\mu g\ ml^{-1}$). The cultures were grown shaking at 37 °C to A_{600} ~ 0.7 and H_6-*Sl*PatA synthesis was induced with IPTG (0.5 mM). Upon induction, the cultures were grown overnight at 30°C. Cells were harvested at 6000 × g for 10 min at 4°C in a Avanti J-2 XPI centrifuge fitted with rotor JLA-8.1000 (Beckman Coulter). Cell pellets were resuspended in 30 ml cold His-Bind buffer (buffer A) [tris(hydroxymethyl)aminomethane-HCl (Tris-HCl) buffer (50 mM, pH 8), NaCl (500 mM)], and imidazole (5 mM)) containing phenylmethanesulfonylfluoride (PMSF, 1 mM). Cells were placed on ice and lysed by sonication for 2 min (2-s pulse followed by 4 s of cooling) at level 7 in a model 550 sonic dismembrator (Fisher). The extract was cleared by centrifugation at 4°C for 30 min at 43,367×*g*. Clarified cell extract was loaded onto a 1 ml HisTrap FF column (GE Healthcare) connected to a computer-controlled ÄKTA fast protein liquid chromatography (FPLC) system. Unbound proteins were eluted off the column by extensive washing with buffer A.

A 10-ml wash step with 90% buffer A and 10% buffer B [Tris-HCl buffer (50 mM, pH 8), NaCl (500 mM), and imidazole (250 mM)] was applied to the column a prior to a 10-ml linear gradient 10–100% Buffer B. All fractions containing H_6-*Sl*PatA were combined. rTEV protease was added to H_6-*Sl*PatA and the *Sl*PatA/rTEV mixture was incubated at room temperature for 3 h. PMSF was added to the protein mixture and incubated 15 min at room temperature. The *Sl*PatA/rTEV mixture was dialyzed at 4°C against buffer C (Tris-HCl (50 mM, pH 8), NaCl (500 mM)) twice for 3 hours and again against buffer C containing imidazole (5 mM) for 12 h. After cleavage and dialysis, protein mixtures were passed over the 1-ml HisTrap column using the buffers described above. Cleaved *Sl*PatA was desorbed from the resin using a 50 ml wash step with 97% buffer A and 3% Buffer B prior to a 25-ml linear gradient 3–100% Buffer B. Purified *Sl*PatA was analyzed by SDS-PAGE. Fractions containing *Sl*PatA were pooled together. *Sl*PatA was stored in Tris-Cl buffer (50 mM, pH 8.0) containing NaCl (100 mM) and glycerol (20%, v/v). *Sl*PatA concentration was determined by measuring absorbance at 280 nm. The molar extinction coefficient used to calculate *Sl*PatA concentration was 57,760 $M^{-1}cm^{-1}$.

***Sl*Acs and *Sl*AacS purification—**Plasmids containing *S. lividans acs* or *aacS* were transformed with pRARE2 (EMD Millipore) into a Δ*pat* derivative of C41λ(DE3) (JE9314) to prevent acetylation prior to overproduction. The resulting strains were grown overnight and sub-cultured 1:100 (v/v) into 2 liters of LB containing ampicillin (100 μg ml^{-1}) and chloramphenicol (12.5 μg ml^{-1}). The cultures were grown shaking at 37 °C to A_{600} ~ 0.7 and protein synthesis was induced with IPTG (0.25 mM). Upon induction, the cultures were grown overnight at 30°C. *Sl*Acs and *Sl*AacS proteins were purified and stored as described above with modifications. During the first purification step, a 10-ml wash step with 94% buffer A and 6% buffer B was applied to the column a prior to a 10-ml linear gradient 6–100% buffer B. *Sl*Acs and *Sl*AacS proteins did not adsorb to the column and were present in the flow-through fractions. The molar extinction coefficient used to calculate protein concentrations were 135,455 cm^{-1} M^{-1} for *Sl*Acs and 142,320 cm^{-1} M^{-1} for *Sl*AacS.

***Se*Acs purification—**Plasmid pACS10 was transformed into a Δ*pat* derivative of C41λ(DE3) (JE9314). The resulting strain was grown overnight and sub-cultured 1:100 (v/v) into 2 liters of LB containing ampicillin (100 μg ml^{-1}). The culture was grown shaking at 37 °C to A_{600} ~ 0.7 and protein synthesis was induced with IPTG (0.25 mM). Upon induction, the cultures were grown overnight at 30°C. *Se*Acs was purified and stored as described (Starai et al., 2002).

In vitro acyl-CoA synthetase assays

*Sl*AacS activity was measured using an NADH-consuming assay (Garrity et al., 2007, Crosby et al., 2010, Fukui *et al.*, 1982, Ito et al., 1984). *R*eactions (100 μl total volume) contained HEPES buffer (50 mM, pH 7.5), TCEP (1 mM), ATP (2.5 mM) CoA (0.5 mM), $MgCl_2$ (5 mM), KCl (1 mM), phosphoenolpyruvate (3 mM), NADH (0.1 mM), pyruvate kinase (1 U), myokinase (5 U), lactate dehydrogenase (1.5 U) and either acetoacetate, β-hydroxybutyrate, butyrate, isovalarate, malonate, crotonate, isobutyrate, succinate, propionate, or acetate (0.2 mM). Reactions were started by the addition of *Sl*AacS (15 nM). The absorbance at 340 nm was monitored in a 96-well plate using the Spectramax Plus UV-visible spectrophotometer (Molecular Devices). Enzyme activities were calculated as described (Garrity et al., 2007). Specific activity data are presented with standard deviations from triplicate experiments.

HPLC separation and mass spectral analysis of *Sl*AacS reaction product

To determine the molecular mass of the *Sl*AacS product, *Sl*AacS was incubated in the presence of CoA, ATP, and acetoacetate, described above, in a final volume of 1 mL.

*Sl*AacS was removed from reactions by filtration using Amicon Ultracel centrifugal filters (3-KDa molecular mass size exclusion). Filtrates containing reaction products and reagents were separated by analytical by reverse-phase ion-pair HPLC using a Beckman Coulter System Gold 126 system equipped with a Phenomenex Synergi Hydro-RP (150 by 4.5 mm, 5 micron particle size, 2.5 ml column volume) column at a flow rate of 1 mL min^{-1}. The solvent system was previously described (Horswill & Escalante-Semerena, 2002, Kawamoto *et al.*, 1998) Briefly, the column was equilibrated with buffer A (100 mM KH2P04, 2 mM tetra-butyl ammonium bromide (TBAB), 15% CH_3CN, pH 3.3). Sample was injected onto the column and washed with buffer A for 5 min. Acetoacetyl-CoA was eluted by a 10-min linear gradient from buffer A to buffer B (100 mM KH2P04, 2 mM TBAB, 35% CH_3CN, pH 3.3). TCEP was added to each sample to a final concentration of 2 mM before injection. Compounds eluted with the following retention times: CoA, 4.7 min; ATP, 2.6 min; AMP, 2.6 min, Acetoacetyl-CoA, 7.3 min. The sample containing acetoacetyl-CoA that eluted from 7 to 9 min was dried under vacuum using an Eppendorf Vacufuge plus concentrator operating at room temperature. The dried sample was resuspended in dH_2O and applied onto a C_{18} Sep-Pak (Waters) previously conditioned with 10 mL of 100% methanol followed by 10 mL of dH_2O. Acetoacetyl-CoA that bound to the column was washed with 10 mL of dH_2O before elution with 100% methanol. Acetoacetyl-CoA dissolved in methanol was concentrated under vacuum. The pellet was resuspended in dH_2O form mass determination by mass spectrometry. The sample as analyzed on a Bruker Autoflex Matrix Assisted Laser Desorption/Ionization-Time-of-Flight mass spectrometer scanning 80–2275 m/z using 300 shots of nitrogen laser in delayed extraction and positive reflectron mode summed together to form the mass spectrum. Matrix for the analysis was dihydroxybenzoate (15 mg/ml, Sigma) in a 1:1 solution of water: 0.1% TFA, CH_3CN (v/v).

In vitro protein acetylation assay

Protein acetylation was observed using radiolabeled Ac-CoA as described (Starai & Escalante-Semerena, 2004, Tucker & Escalante-Semerena, 2010, Crosby et al., 2010). Acetylation reactions contained 2(Bis(2-hydroxyethyl)imino)-2-(hydroxymethyl)-1,3-propanediol (Bis-Tris-HCl) buffer (50 mM, pH 6.0), [1-^{14}C]-Ac-CoA (20 μM), acyl-CoA synthetase (3 μM), glycerol (10%, v/v), and *Sl*PatA (1 μM). Reactions (10 μl total volume) were incubated for min at 30°C. Samples (5 μl) were resolved using SDS-PAGE (Laemmli, 1970) and proteins were visualize by Coomassie Blue staining. Gels were dried and exposed 16 h to a multipurpose phosphor screen (Packard). Labeled proteins were visualized using a Typhoon FLA 9000 Variable Mode Imager (GE Healthcare) equipped with ImageQuant TL software (GE Healthcare).

The effect of acetylation on activity of *Sl*AacS, *Sl*Acs, and *Se*Acs activity was determined as described (Crosby et al., 2010) with modifications. *Sl*AacS (3μM) was incubated with *Sl*PatA (1 μM) and 50 μM Ac-CoA for 90 minutes at 30°C using the buffer system described above. At 0, 15, 30, 60, and 90 min time points, reactions were diluted 1:20 into 50 mM HEPES buffer pH 7.5 at 4°C. *Sl*AacS, *Sl*Acs, and *Se*Acs activity were measured as described above using the appropriate organic acid substrate.

In vitro deacetylation assays

Acetylated *Sl*AacS was deacetylated with *Salmonella enterica* $CobB_S$ as described (Tucker & Escalante-Semerena, 2010). *In vitro* acetylated *Sl*AacS (3 μM, radiolabeled or non-radiolabeled) was incubated with *Se*$CobB_S$ (3 μM) in deacetylation buffer containing 4-(2-hydroxyethyl)-1-piperazineethanesulfonic acid (HEPES, 50 mM, pH 7.0), NAD^+ (1 mM) for 60 min at 37°C (25 μl reaction volume). Reaction mixture samples (5 μl) were resolved by SDS-PAGE, and subjected to phosphor imaging analysis to assess the acetylation state of

*Sl*AacS after incubation with *Se*CobB$_S$. *Sl*AacS activity of the non-radiolabeled reactions was measured using the CoA synthetase assay described above.

Purification or *Sl*AacS from *S. lividans*

Plasmid p*Sl*AacS5 was introduced into *S. lividans* TK24 and *S. lividans* Δ*patA* (JE16707) by polyethyleneglycol (PEG)-assisted protoplast transformation as described (Kieser et al., 2000b, Kieser *et al.*, 2000a) to generate JE16731 and JE16821 (Table S1), respectively. Cells were plated on R2YE and grown at 30°C for 16 hours. Plates were flooded with thiostrepton (10 μg ml^{-1} final concentration) and incubated 3 days at 30°C to select for strains harboring p*Sl*AacS5. *S. lividans* strains harboring the p*Sl*AacS5 plasmid encoding H$_6$-*Sl*AacS were grown in 30 ml YEME + thiostrepton for 5 days. Cells were harvested by centrifugation at 2000 × *g* for 10 min at 4°C. Cell mass was measured and cells were resuspended in an equal volume of NMMP. Approximately 0.1 g of cells were inoculated into 250 ml NMMP + thiostrepton supplemented with acetoacetate (10 mM). Strains were grown for 24 h at 30°C with shaking. Cells were harvested as described above and washed twice with 50 ml wash buffer containing Tris-HCl buffer (50 mM, pH 8.0) and NaCl (500 mM). Cells pellets were resuspended in 30 ml buffer A (described above) supplemented with PMSF (1 mM), Sigma protease inhibitor cocktail for histidine-tagged proteins (100 μl), and lysozyme (1 mg ml^{-1}). Cells were lysed by sonication and cell debris was removed by centrifugation. H$_6$-*Sl*AacS was purified using 250 μl HisPur Ni-NTA resin (Pierce). Using the same buffer system described for *Sl*AacS above. *Sl*AacS-containing fractions were combined and dialyzed overnight into HEPES buffer (50 mM, pH 7.5) containing NaCl (150 mM) and glycerol (20%, v/v).

*Sl*AacS of SlAacS activity was assessed using the deacetylation reaction described above. *Sl*AacS (1 μM) purified from JE16731 and JE16821 (Table S1) were incubated with or without *Se*CobB$_S$ as described in the above section for 1 h at 37°C. A sample for the deacetylation reaction mixtures was used to assess *Sl*AacS activity. The concentration of *SlAacS* in the CoA synthetase activity assay was 25 nM.

Western blot analysis of H$_6$-*Sl*AacS purified from *S. lividans*

Purified *Sl*AacS or in vitro acetylated *Sl*AacS were resolved along with H$_6$-*Sl*AacS purified from *S. lividans* strains JE16731 and JE16821 (Table 1) (2 ug each) using SDS-PAGE and transferred to a polyvinylidene fluoride (PVDF) membrane (Millipore). Total protein was visualized by staining 15 seconds in Ponceau-S staining solution (0.1% (w/v) Ponceau S in 5% (v/v) acetic acid) and de-staining with distilled water. After extensive de-staining, the PVDF membranes were probed with polyclonal rabbit α-acetylated lysine antibodies (1:1,700; Calbiochem) as primary antibody and goat α-rabbit immunoglobulin G conjugated to calf intestinal alkaline phosphatase (Pierce) (1:10,000) as secondary antibody to detect *Sl*AacS^{Ac}. Signal was detected using nitro-blue tetrazolium chloride and 5-bromo-4-chloro-3′-indolylphosphate *p*-toluidine salt (NBT-BCIP) 1-Step Solution according to the manufacturer's instructions (Pierce).

Determination of the *Sl*AacS acetylation site by mass spectrometry

To determine the identity of the *in vivo* modification of *Sl*AacS, H$_6$-*Sl*AacS purified from *S. lividans* was resolved by SDS-PAGE and the band corresponding to *Sl*AacS was excised. “In Gel” digestion and mass spectrometric analysis was done at the Mass Spectrometry Facility [Biotechnology Center, University of Wisconsin-Madison]. The digestion was performed as outlined on the website: http://www.biotech.wisc.edu/facilities/massspec/protocols/ingelprotocol.

Peptides were analyzed by nanoLC-MS/MS using the Agilent 1100 nanoflow system (Agilent, Palo Alto, CA) connected to a hybrid linear ion trap-orbitrap mass spectrometer (LTQ-Orbitrap, Thermo Fisher Scientific, Bremen, Germany) equipped with a nanoelectrospray ion source (Proxeon Biosystems, Odense, Denmark). Chromatography of peptides prior to mass spectral analysis was accomplished using C18 reverse phase HPLC trap column (Zorbax 300SB-C18, 5μM, 5×0.3mm, Agilent) and capillary emitter column (in-house packed with MAGIC C18, 3 μM, 15×0.075mm, Michrom Bioresources, Inc.) onto which 8μl of extracted peptides were automatically loaded. NanoHPLC system delivered solvents A: 0.1% (v/v) formic acid in water, and B: 95% (v/v) acetonitrile, 0.1% (v/v) formic acid at either 10 μL/min, to load sample, or 0.20 μL/min, to elute peptides directly into the nano-electrospray over a 60 minutes 1% (v/v) B to 60% (v/v) B followed by 10 minute 60% (v/v) B to 100% (v/v) B gradient. As peptides eluted from the HPLC-column/electrospray source survey MS scans were acquired in the orbitrap with a resolution of 100 000 and up to 5 most intense peptides per scan were fragmented and detected in the ion trap over the 400 to 2000 m/z; redundancy was limited by dynamic exclusion. Raw MS/MS data were converted to mgf file format using Trans Proteomic Pipeline (Seattle Proteome Center, Seattle, WA). Resulting mgf files were used to search user defined amino acid sequence database using in-house Mascot search engine 2.2.07 (Matrix Science, London, UK) with Cysteine carbamidomethylation as fixed modification and Lysine acetylation, methionine oxidation, and Asparigine/Glutamine deamidation as variable modifications. Peptide mass tolerance was set at 20 ppm and fragment mass at 0.8 Da. Protein annotations and significance of identification was done with help of Scaffold software (version 3.6.1, Proteome Software Inc., Portland, OR). Peptide identifications were accepted if they could be established at greater than 95.0% probability as specified by the Peptide Prophet algorithm (Keller *et al.*, 2002). Protein identifications were accepted if they could be established at greater than 95.0% probability and contained at least 2 identified peptides. Protein probabilities were assigned by the Protein Prophet algorithm (Nesvizhskii *et al.*, 2003). Proteins that contained similar peptides and could not be differentiated based on MS/MS analysis alone were grouped to satisfy the principles of parsimony.

Supplementary Material

Refer to Web version on PubMed Central for supplementary material.

Acknowledgments

This work was supported by USPHS grant R01-GM62203 to J.C.E.-S. A.C.T. was supported by the NIH Molecular Biosciences Training Grant T32-GM07215.

We thank Michael Thomas (UW – Madison) for providing *Streptomyces lividans* TK24 and plasmids pKC1139 and pSE34. We also thank Michael Thomas, John Barkei, and Matt McMahon for valuable advice about working with *S. lividans*.

References

Anderson AJ, Dawes EA. Occurrence, metabolism, metabolic role, and industrial uses of bacterial polyhydroxyalkanoates. Microbiol. Rev. 1990; 54:450–472. [PubMed: 2087222]

Beck K, Brodsky B. Supercoiled protein motifs: the collagen triple-helix and the alpha-helical coiled coil. J. Struct. Biol. 1998; 122:17–29. [PubMed: 9724603]

Berkowitz D, Hushon JM, Whitfield HJ Jr. Roth J, Ames BN. Procedure for identifying nonsense mutations. J. Bacteriol. 1968; 96:215–220. [PubMed: 4874308]

Bertani G. Studies on lysogenesis. I. The mode of phage liberation by lysogenic *Escherichia coli*. J. Bacteriol. 1951; 62:293–300. [PubMed: 14888646]

Bierman M, Logan R, O'Brien K, Seno ET, Rao RN, Schoner BE. Plasmid cloning vectors for the conjugal transfer of DNA from *Escherichia coli* to *Streptomyces* spp. Gene. 1992; 116:43–49. [PubMed: 1628843]

Blommel PG, Fox BG. A combined approach to improving large-scale production of tobacco etch virus protease. Protein Expr. Purif. 2007; 55:53–68. [PubMed: 17543538]

Buckley BM, Williamson DH. Acetoacetate and brain lipogenesis: developmental pattern of acetoacetyl-coenzyme A synthetase in the soluble fraction of rat brain. Biochem. J. 1973; 132:653–656. [PubMed: 4724596]

Cai GQ, Driscoll BT, Charles TC. Requirement for the enzymes acetoacetyl coenzyme A synthetase and poly-3-hydroxybutyrate (PHB) synthase for growth of *Sinorhizobium meliloti* on PHB cycle intermediates. J. Bacteriol. 2000; 182:2113–2118. [PubMed: 10735852]

Chan CH, Garrity J, Crosby HA, Escalante-Semerena JC. In Salmonella enterica, the sirtuin-dependent protein acylation/deacylation system (SDPADS) maintains energy homeostasis during growth on low concentrations of acetate. Mol. Microbiol. 2011; 80:168–183. [PubMed: 21306440]

Charalambous BM, Keen JN, McPherson MJ. Collagen-like sequences stabilize homotrimers of a bacterial hydrolase. EMBO J. 1988; 7:2903–2909. [PubMed: 2846288]

Chater KF. *Streptomyces* inside-out: a new perspective on the bacteria that provide us with antibiotics. Philos. Trans. R. Soc. Lond. B. Biol. Sci. 2006; 361:761–768. [PubMed: 16627293]

Choudhary C, Kumar C, Gnad F, Nielsen ML, Rehman M, Walther T, Olsen JV, Mann M. Lysine acetylation targets protein complexes and co-regulates major cellular functions. Science. 2009; 325:834–840. [PubMed: 19608861]

Courtois S, Cappellano CM, Ball M, Francou FX, Normand P, Helynck G, Martinez A, Kolvek SJ, Hopke J, Osburne MS, August PR, Nalin R, Guerineau M, Jeannin P, Simonet P, Pernodet JL. Recombinant environmental libraries provide access to microbial diversity for drug discovery from natural products. Appl. Environ. Microbiol. 2003; 69:49–55. [PubMed: 12513976]

Crosby HA, Heiniger EK, Harwood CS, Escalante-Semerena JC. Reversible N(epsilon)-lysine acetylation regulates the activity of acyl-CoA synthetases involved in anaerobic benzoate catabolism in *Rhodopseudomonas palustris*. Mol. Microbiol. 2010; 76:874–888. [PubMed: 20345662]

Crosby HA, Pelletier DA, Hurst GB, Escalante-Semerena JC. System-wide studies of N-lysine acetylation in *Rhodopseudomonas palustris* reveal substrate specificity of protein acetyltransferases. J. Biol. Chem. 2012; 287:15590–15601. [PubMed: 22416131]

Datsenko KA, Wanner BL. One-step inactivation of chromosomal genes in *Escherichia coli* K-12 using PCR products. Proc. Natl. Acad. Sci. USA. 2000; 97:6640–6645. [PubMed: 10829079]

Elion, EA.; Marina, P.; Yu, L. Constructing recombinant DNA molecules by PCR. In: Ausubel, FM.; Brent, RER.; Kingston, DD.; Moore, JG.; Seidman, JA.; Smith, a.; Struhl, K., editors. Current protocols in molecular biology. Greene Publishing Associates & Wiley Interscience; New York, N.Y.: 2007. p. Unit 3.17.11-13.17.12.

Erb TJ, Berg IA, Brecht V, Muller M, Fuchs G, Alber BE. Synthesis of C5-dicarboxylic acids from C2-units involving crotonyl-CoA carboxylase/reductase: the ethylmalonyl-CoA pathway. Proceedings of the National Academy of Sciences of the United States of America. 2007; 104:10631–10636. [PubMed: 17548827]

Figurski DH, Helinski DR. Replication of an origin-containing derivative of plasmid RK2 dependent on a plasmid function provided in trans. Proc. Natl. Acad. Sci. 1979; 76:1648–1652. [PubMed: 377280]

Fukui T, Ito M, Tomita K. Purification and characterization of acetoacetyl-CoA synthetase from *Zoogloea ramigera* I-16-M. Eur. J. Biochem. 1982; 127:423–428. [PubMed: 7140777]

Gardner JG, Grundy FJ, Henkin TM, Escalante-Semerena JC. Control of acetyl-coenzyme A synthetase (AcsA) activity by acetylation/deacetylation without NAD(+) involvement in *Bacillus subtilis*. J. Bacteriol. 2006; 188:5460–5468. [PubMed: 16855235]

Garrity J, Gardner JG, Hawse W, Wolberger C, Escalante-Semerena JC. N-lysine propionylation controls the activity of propionyl-CoA synthetase. J. Biol. Chem. 2007; 282:30239–30245. [PubMed: 17684016]

Geelen MJ, Lopes-Cardozo M, Edmond J. Acetoacetate: a major substrate for the synthesis of cholesterol and fatty acids by isolated rat hepatocytes. FEBS Lett. 1983; 163:269–273. [PubMed: 6641943]

Gu T, Orita S, Han M. *Caenorhabditis elegans* SUR-5, a novel but conserved protein, negatively regulates LET-60 Ras activity during vulval induction. Mol. Cell. Biol. 1998; 18:4556–4564. [PubMed: 9671465]

Guzman LM, Belin D, Carson MJ, Beckwith J. Tight regulation, modulation, and high-level expression by vectors containing the arabinose PBAD promoter. J. Bacteriol. 1995; 177:4121–4130. [PubMed: 7608087]

Hay RW, Bond MA. Kinetics of decarboxylation of acetoacetic acid. Aust. J. Chem. 1967; 20:1823–1828.

Horswill AR, Escalante-Semerena JC. Characterization of the propionyl-CoA synthetase (PrpE) enzyme of *Salmonella enterica*: Residue Lys592 is required for propionyl-AMP synthesis. Biochemistry. 2002; 41:2379–2387. [PubMed: 11841231]

Hulmes DJ. The collagen superfamily - diverse structures and assemblies. Essays Biochem. 1992; 27:49–67. [PubMed: 1425603]

Ikeuchi Y, Kitahara K, Suzuki T. The RNA acetyltransferase driven by ATP hydrolysis synthesizes N4-acetylcytidine of tRNA anticodon. Embo J. 2008; 27:2194–2203. [PubMed: 18668122]

Ito M, Fukui T, Kamokari M, Saito T, Tomita K. Purification and characterization of acetoacetyl-CoA synthetase from rat liver. Biochim. Biophys. Acta. 1984; 794:183–193. [PubMed: 6539623]

Jenkins LS, Nunn WD. Genetic and molecular characterization of the genes involved in short-chain fatty acid degradation in *Escherichia coli*: the *ato* system. J. Bacteriol. 1987; 169:42–52. [PubMed: 3025185]

Kawamoto S, Ochi K. Comparative ribosomal protein (L11 and L30) sequence analyses of several *Streptomyces* spp. commonly used in genetic studies. Int. J. Syst. Bacteriol. 1998; 48:597–600. [PubMed: 9731302]

Kawamoto Y, Shinozuka K, Kunitomo M, Haginaka J. Determination of ATP and its metabolites released from rat caudal artery by isocratic ion-pair reversed-phase high-performance liquid chromatography. Anal. Biochem. 1998; 262:33–38. [PubMed: 9735145]

Keller A, Nesvizhskii AI, Kolker E, Aebersold R. Empirical statistical model to estimate the accuracy of peptide identifications made by MS/MS and database search. Anal. Chem. 2002; 74:5383–5392. [PubMed: 12403597]

Khan SR, Gaines J, Roop RM 2nd, Farrand SK. Broad-host-range expression vectors with tightly regulated promoters and their use to examine the influence of TraR and TraM expression on Ti plasmid quorum sensing. Appl. Environ. Microbiol. 2008; 74:5053–5062. [PubMed: 18606801]

Kieser, T.; Bibb, MJ.; Buttner, MJ.; Chater, K.; Hopwood, DA. Practical *Streptomyces* Genetics. John Innes Foundation; Norwich, England: 2000a. Growth and preservation of *Streptomyces*; p. 43-62.

Kieser, T.; Bibb, MJ.; Buttner, MJ.; Chater, K.; Hopwood, DA. Practical *Streptomyces* Genetics. John Innes Foundation; Norwich, England: 2000b. Introduction of DNA into *Streptomyces*; p. 229-252.

Kieser, T.; Bibb, MJ.; Buttner, MJ.; Chater, K.; Hopwood, DA. Practical *Streptomyces* Genetics. John Innes Foundation; Norwich, England: 2000c. Media, buffers, and suppliers; p. 405-420.

Kim SC, Sprung R, Chen Y, Xu Y, Ball H, Pei J, Cheng T, Kho Y, Xiao H, Xiao L, Grishin NV, White M, Yang XJ, Zhao Y. Substrate and functional diversity of lysine acetylation revealed by a proteomics survey. Mol. Cell. 2006; 23:607–618. [PubMed: 16916647]

Laemmli UK. Cleavage of structural proteins during the assembly of the head of bacteriophage T4. Nature. 1970; 227:680–685. [PubMed: 5432063]

Lee HJ, Lang PT, Fortune SM, Sassetti CM, Alber T. Cyclic AMP regulation of protein lysine acetylation in *Mycobacterium tuberculosis*. Nat. Struct. Mol. Biol. 2012

Lewis RA, Laing E, Allenby N, Bucca G, Brenner V, Harrison M, Kierzek AM, Smith CP. Metabolic and evolutionary insights into the closely-related species S*treptomyces coelicolor* and *Streptomyces lividans* deduced from high-resolution comparative genomic hybridization. BMC Genomics. 2010; 11:682. [PubMed: 21122120]

Martinez A, Kolvek SJ, Yip CL, Hopke J, Brown KA, MacNeil IA, Osburne MS. Genetically modified bacterial strains and novel bacterial artificial chromosome shuttle vectors for constructing

environmental libraries and detecting heterologous natural products in multiple expression hosts. Appl. Environ. Microbiol. 2004; 70:2452–2463. [PubMed: 15066844]

McMahon MD, Guan C, Handelsman J, Thomas MG. Metagenomic analysis of *Streptomyces lividans* reveals host-dependent functional expression. Appl. Environ. Microbiol. 2012; 78:3622–3629. [PubMed: 22427497]

Mikulik K, Felsberg J, Kudrnacova E, Bezouskova S, Setinova D, Stodulkova E, Zidkova J, Zidek V. CobB1 deacetylase activity in *Streptomyces coelicolor*. Biochem. Cell Biol. 2012; 90:179–187. [PubMed: 22300453]

Nambi S, Basu N, Visweswariah SS. Cyclic AMP-regulated protein lysine acetylases in mycobacteria. J. Biol. Chem. 2010; 285:24313–24323. [PubMed: 20507997]

Nesvizhskii AI, Keller A, Kolker E, Aebersold R. A statistical model for identifying proteins by tandem mass spectrometry. Anal. Chem. 2003; 75:4646–4658. [PubMed: 14632076]

Pauli G, Overath P. *ato* Operon: a highly inducible system for acetoacetate and butyrate degradation in *Escherichia coli*. Eur. J. Biochem. 1972; 29:553–562. [PubMed: 4563344]

Reizer J, Saier MH Jr. Modular multidomain phosphoryl transfer proteins of bacteria. Curr. Opin. Struct. Biol. 1997; 7:407–415. [PubMed: 9204284]

Rocco CJ, Dennison KL, Klenchin VA, Rayment I, Escalante-Semerena JC. Construction and use of new cloning vectors for the rapid isolation of recombinant proteins from *Escherichia coli*. Plasmid. 2008; 59:231–237. [PubMed: 18295882]

Sánchez LB, Galperin MY, Muller M. Acetyl-CoA synthetase from the amitochondriate eukaryote Giardia lamblia belongs to the newly recognized superfamily of acyl-CoA synthetases (Nucleoside diphosphate-forming). J. Biol. Chem. 2000; 275:5794–5803. [PubMed: 10681568]

Seow KT, Meurer G, Gerlitz M, Wendt-Pienkowski E, Hutchinson CR, Davies J. A study of iterative type II polyketide synthases, using bacterial genes cloned from soil DNA: a means to access and use genes from uncultured microorganisms. J. Bacteriol. 1997; 179:7360–7368. [PubMed: 9393700]

Shaw KJ, Rather PN, Hare RS, Miller GH. Molecular genetics of aminoglycoside resistance genes and familial relationships of the aminoglycoside-modifying enzymes. Microbiol. Rev. 1993; 57:138–163. [PubMed: 8385262]

Shirling EB, Gottlieb D. Methods for characterization of *Streptomyces* species. Int. J. Syst. Bacteriol. 1966; 16:313–340.

Soppa J. Protein acetylation in archaea, bacteria, and eukaryotes. Archaea. 2010; 2010

Spange S, Wagner T, Heinzel T, Kramer OH. Acetylation of non-histone proteins modulates cellular signalling at multiple levels. Int. J. Biochem. Cell. Biol. 2009; 41:185–198. [PubMed: 18804549]

Staack H, Binstock JF, Schulz H. Purification and properties of a pig heart thiolase with broad chain length specificity and comparison of thiolases from pig heart and *Escherichia coli*. J. Biol. Chem. 1978; 253:1827–1831. [PubMed: 344310]

Starai VJ, Celic I, Cole RN, Boeke JD, Escalante-Semerena JC. Sir2-dependent activation of acetyl-CoA synthetase by deacetylation of active lysine. Science. 2002; 298:2390–2392. [PubMed: 12493915]

Starai VJ, Escalante-Semerena JC. Identification of the protein acetyltransferase (Pat) enzyme that acetylates acetyl-CoA synthetase in *Salmonella enterica*. J. Mol. Biol. 2004; 340:1005–1012. [PubMed: 15236963]

Takenoya M, Nikolakakis K, Sagermann M. Crystallographic insights into the pore structures and mechanisms of the EutL and EutM shell proteins of the Eut-BMC. J. Bacteriol. 2010; 192:6056–6063. [PubMed: 20851901]

Thao S, Chen CS, Zhu H, Escalante-Semerena JC. N(epsilon)-Lysine acetylation of a bacterial transcription factor inhibits its DNA-binding activity. PLoS ONE. 2010; 5:e15123. [PubMed: 21217812]

Thao S, Escalante-Semerena JC. Biochemical and thermodynamic analyses of *Salmonella enterica* Pat, a multidomain, multimeric N(epsilon)-lysine acetyltransferase involved in carbon and energy metabolism. mBio. 2011a; 2:e00216–00211. [PubMed: 22010215]

Thao S, Escalante-Semerena JC. Control of protein function by reversible N(epsilon)-lysine acetylation in bacteria. Curr. Opin. Microbiol. 2011b; 14:200–204. [PubMed: 21239213]

Tsang AW, Escalante-Semerena JC. CobB, a new member of the SIR2 family of eucaryotic regulatory proteins, is required to compensate for the lack of nicotinate mononucleotide:5,6-dimethylbenzimidazole phosphoribosyltransferase activity in *cobT* mutants during cobalamin biosynthesis in *Salmonella typhimurium* LT2. J. Biol. Chem. 1998; 273:31788–31794. [PubMed: 9822644]

Tucker AC, Escalante-Semerena JC. Biologically active isoforms of CobB sirtuin deacetylase in *Salmonella enterica* and *Erwinia amylovora*. J. Bacteriol. 2010; 192:6200–6208. [PubMed: 20889757]

Vetting MW, Carvalho L. P. S. d. Yu M, Hegde SS, Magnet S, Roderick SL, Blanchard JS. Structure and functions of the GNAT superfamily of acetyltransferases. Arch. Biochem. Biophys. 2005; 433:212–226. [PubMed: 15581578]

Ward JM, Janssen GR, Kieser T, Bibb MJ, Buttner MJ. Construction and characterisation of a series of multi-copy promoter-probe plasmid vectors for *Streptomyces* using the aminoglycoside phosphotransferase gene from Tn*5* as indicator. Mol. Gen. Genet. 1986; 203:468–478. [PubMed: 3018431]

Weinert BT, Wagner SA, Horn H, Henriksen P, Liu WR, Olsen JV, Jensen LJ, Choudhary C. Proteome-wide mapping of the *Drosophila* acetylome demonstrates a high degree of conservation of lysine acetylation. Science signaling. 2011; 4:ra48. [PubMed: 21791702]

Xu H, Hegde SS, Blanchard JS. Reversible acetylation and inactivation of *Mycobacterium tuberculosis* acetyl-CoA synthetase is dependent on cAMP. Biochemistry. 2011; 50:5883–5892. [PubMed: 21627103]

Xu Y, Keene DR, Bujnicki JM, Hook M, Lukomski S. Streptococcal Scl1 and Scl2 proteins form collagen-like triple helices. J. Biol. Chem. 2002; 277:27312–27318. [PubMed: 11976327]

Yamasaki M, Hasegawa S, Kitani T, Hidai K, Fukui T. Differential effects of obesity on acetoacetyl-CoA synthetase gene in rat adipose tissues. Eur. J. Lipid Sci. Technol. 2007; 109:617–622.

Yu BJ, Kim JA, Moon JH, Ryu SE, Pan JG. The diversity of lysine-acetylated proteins in *Escherichia coli*. J. Microbiol. Biotechnol. 2008; 18:1529–1536. [PubMed: 18852508]

Zhang J, Sprung R, Pei J, Tan X, Kim S, Zhu H, Liu CF, Grishin NV, Zhao Y. Lysine acetylation is a highly abundant and evolutionarily conserved modification in *Escherichia coli*. Mol. Cell. Proteomics. 2009; 8:215–225. [PubMed: 18723842]

Zhao S, Xu W, Jiang W, Yu W, Lin Y, Zhang T, Yao J, Zhou L, Zeng Y, Li H, Li Y, Shi J, An W, Hancock SM, He F, Qin L, Chin J, Yang P, Chen X, Lei Q, Xiong Y, Guan KL. Regulation of cellular metabolism by protein lysine acetylation. Science. 2010; 327:1000–1004. [PubMed: 20167786]

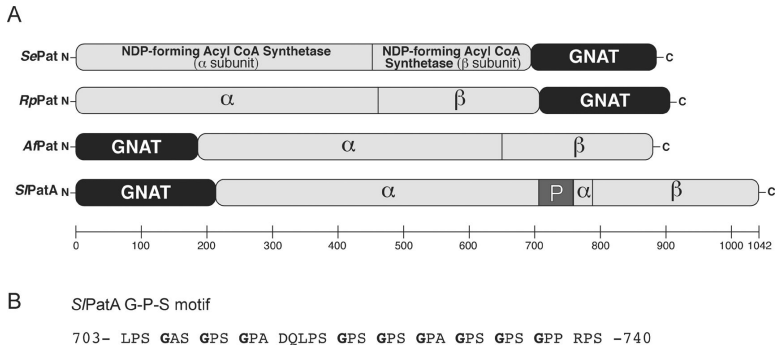

Figure 1. Domain organization of Pat homologues

(A) Pat homologues encode a GNAT domain (black) and large domain that is homologous to NDP-forming acyl-CoA synthetases (light gray). *S. lividans* PatA also contains a proline-rich domain in the large domain (dark gray, denoted by "P"). *Se*Pat, *Salmonella enterica* Pat (NP_461586); *Rp*Pat, *Rhodopseudomonas palustris* Pat (NP_949576); *Af*Pat *Archaeoglobus fulgidus* Pat (NP_070340); *Sl*PatA, *Streptomyces lividans* PatA (ZP_06527997). (B) The degenerate G-P-S motif Leu703-Ser740 in *Sl*PatA.

Tucker & Escalante-Semerena

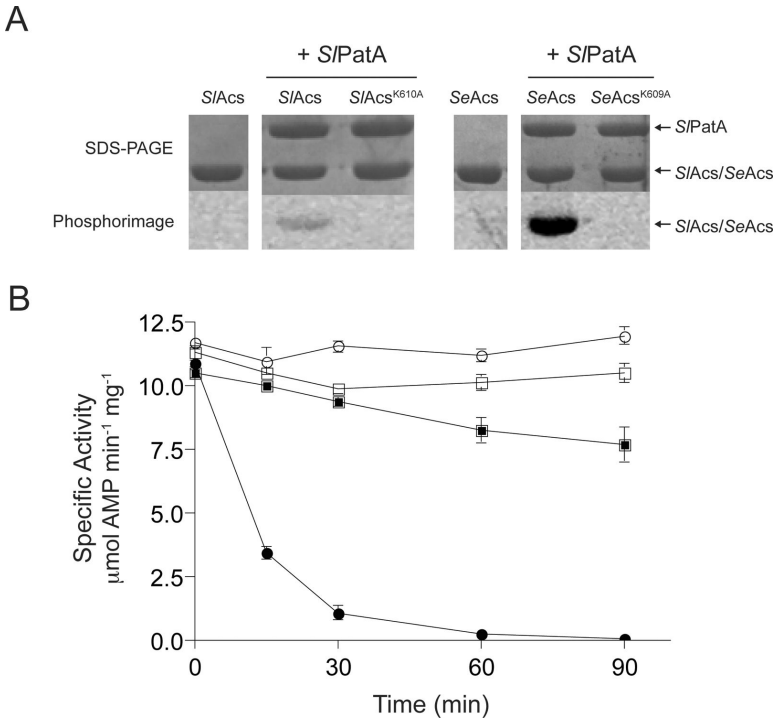

Figure 2. *Sl*PatA acetylates *Sl*Acs from *S. lividans*

(A) *Sl*Acs, *Sl*Acs^{K610A}, *Se*Acs, or *Se*Acs^{K609A} was incubated with [1-^{14}C]-acetyl-CoA in the presence or absence of *Sl*PatA. Proteins were separated by SDS-PAGE and stained with Coomassie Blue to visualize proteins. Acetylation was visualized by phosphor imaging. *Sl*PatA was incubated with *Sl*Acs or *Se*Ac in the presence or absence of unlabeled acetyl-CoA (B). Reactions were carried out with 1:3 molar ratios of *Sl*PatA to *Sl*Acs/*Se*Acs. Sample were diluted and assayed to measure *Sl*Acs/*Se*Acs activity at 0, 15, 30, 60, and 90 min after incubation with *Sl*PatA. *Sl*Acs (squares) and *Se*Acs (circles) activities were measured in and NADH-consumption assay and activities are reported for the reactions containing acetyl-CoA (closed symbols) and the control reactions lacking acetyl-CoA (open symbols). Reactions were carried out in triplicate. Error bars represent standard deviations. Tucker & Escalante-Semerena

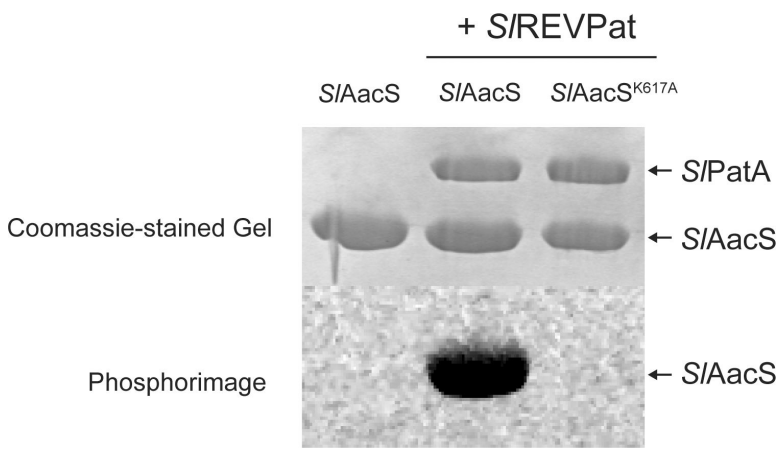

Figure 3. *Sl*PatA acetylates *Sl*AacS from *S. lividans* at the conserved active site lysine

Alignment of *Sl*AacS with known acetylation targets from *S. enterica* (*Se*Acs, encoded by locus STM4275; *Se*PrpE, encoded by locus STM0371), *R. palustris* (*Rp*BadA, encoded by locus RPA0661; *Rp*AliA, encoded by locus RPA0651; *Rp*HbaA, encoded by locus RPA0669; *Rp*PrpE, encoded by locus RPA4504; *Rp*Acs, encoded by locus RPA0211), and *S. lividans* indicates a conserved active site lysine (A). Acetylation of *Sl*AacS and *Sl*AacSK617A was assessed after incubation of proteins with [1-^{14}C]-acetyl-CoA in the presence or absence of *Sl*PatA. Proteins were separated by SDS-PAGE and stained with Coomassie Blue to visualize proteins. Acetylation was visualized by phosphor imaging (B). Tucker & Escalante-Semerena

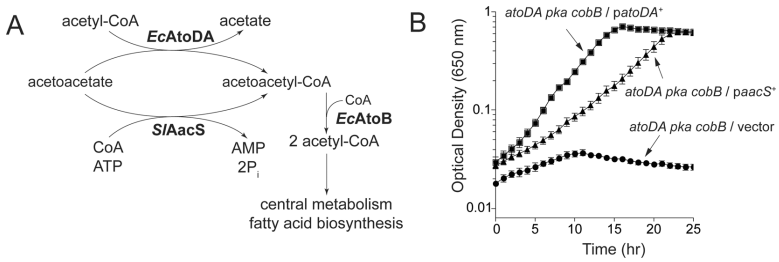

Figure 4. *Sl*AacS can substitute for *Ec*AtoDA in *E. coli* during growth on acetoacetate

Acetoacetate utilization in *E. coli* involves a 2-step conversion from acetoacetate to acetoacetyl CoA and from acetoacetyl-CoA to 2 molecules of acetyl-CoA. *Sl*AacS is predicted by homology to catalyze the conversion of acetatoacetate to acetoacetyl-CoA (A). Growth behavior of *S. enterica* on NCE minimal medium supplemented with acetoacetate (30 mM). Growth experiments were performed at 37°C using a microtiter plate and a microtiter plate reader (Bio-Tek Instruments). Growth experiments were performed in triplicate. Error bars represent standard deviations.

Tucker & Escalante-Semerena

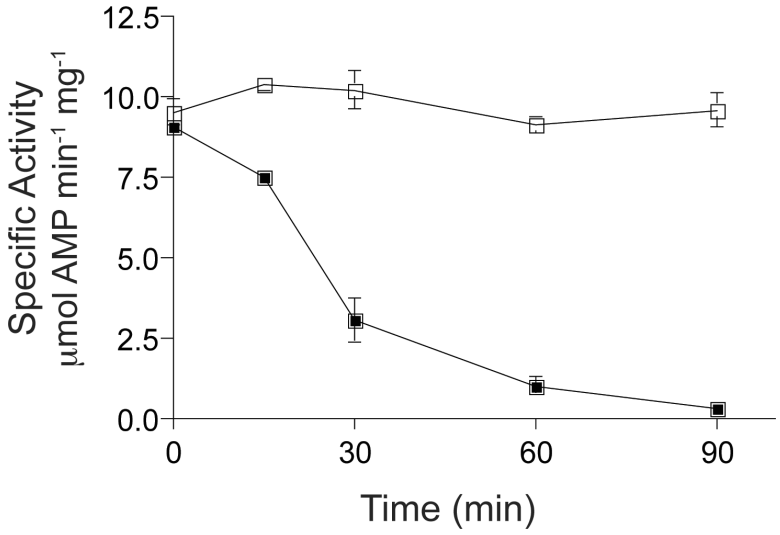

Figure 5. *Sl*PatA acetylation inactivates *Sl*AacS

*Sl*AacS was incubated with *Sl*PatA at a 3:1 molar ratio (*Sl*AacS:*Sl*PatA) in the presence (closed squares) or absence (open squares) of acetyl-CoA. Sample were removed, diluted, and assayed to measure *Sl*Acs/*Se*Acs activity at 0, 15, 30, 60, and 90 min after incubation with *Sl*PatA. *Sl*AacS activity was measured in an NADH-consumption assay. Reactions were carried out in triplicate. Error bars represent standard deviations.

Tucker & Escalante-Semerena

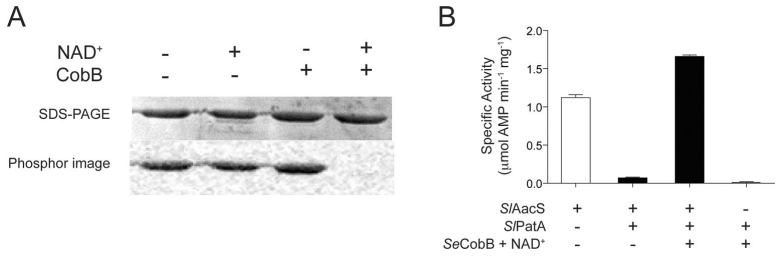

Figure 6. *Sl*AacS is deacetylated and reactivated by a heterologous sirtuin

*A. Sl*AacS previously acetylated by *Sl*PatA with [1-^{14}C]-acetyl-CoA was incubated with the addition of *Se*CobB and/or NAD^+. Proteins were resolved by SDS-PAGE and stained with Coomassie Blue to visualize proteins. Acetylation was visualized by phosphor image. B. *Sl*AacS was incubated in the presence or absence of *Sl*PatA and unlabeled acetyl-CoA and the acetylation reaction was stopped by buffer exchange. *Se*CobB and NAD^+ were added to the reactions and *Sl*AacS activity was measured in triplicate. Error bars represent standard deviations.

Tucker & Escalante-Semerena

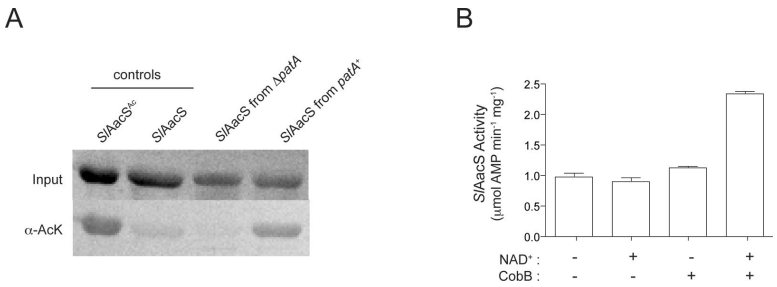

Figure 7. *Sl*AacS is acetylated in vivo in *S. lividans*

(A) H_6-*Sl*AacS was isolated from *S. lividans pat*$^+$ and Δ*patA* strains grown on acetoacetate. Acetylation state of the H_6-*Sl*AacS proteins was analyzed by anti-acetyllysine Western blot analysis. *In vitro* acetylated and nonacetylated *Sl*AacS were used as positive and negative controls, respectively. Total protein was visualized by Ponceau S staining prior to Western blot analysis. (B) H_6-*Sl*AacS isolated from *S. lividans pat*$^+$ and Δ*patA* strains was incubated with *Se*CobB and NAD^+ to assess the affect of deacetylation on H_6-*Sl*AacS activity. For (A) and (B), experiments were conducted on H_6-*Sl*AacS isolated in three independent experiments. Error bars represent standard deviations.

Tucker & Escalante-Semerena

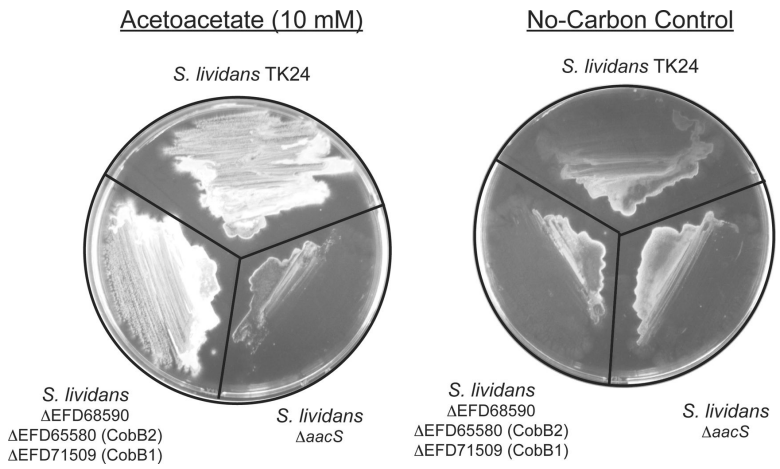

Figure 8. *Sl*AacS is required for growth of *S. lividans* on acetoacetate

Spores from *S. lividans* strains TK24 (wild-type), JE16752 (ΔEFD65580 ΔEFD68590 ΔEFD71509), and JE16758 (Δ*aacS*) were streaked on minimal medium containing acetoacetate (10 mM) or no additional carbon source. Plates were incubated at 30°C for 7 days prior to imaging using a Photodyne digital imaging system.

Tucker & Escalante-Semerena

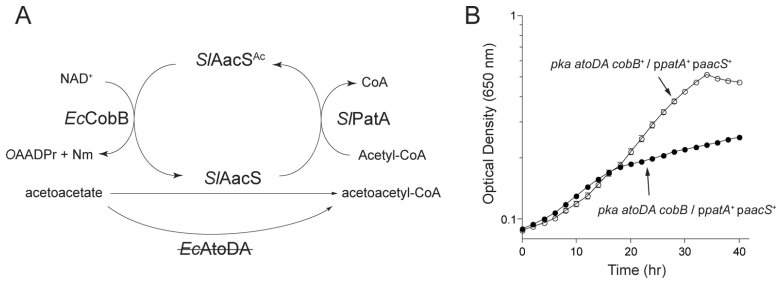

Figure 9. *Sl*PatA modulates growth of *E. coli* on acetoacetate using *Sl*AacS

(A) Schematic of predicted regulation of *E. coli atoDA aacS*$^{+}$ growth on acetoacetate. (B) *E. coli pka atoDA aacS*$^{+}$ strains encoding or lacking *cobB* were grown on NCE minimal medium supplemented with acetoacetate (30 mM) in the presence of *Sl*PatA (p*patA*$^{+}$). Growth experiments were performed at 37°C using a microtiter plate and a microtiter plate reader (Bio-Tek Instruments). Experiments were conducted in triplicate. Error bars represent standard deviations.

Tucker & Escalante-Semerena

Table 1

Comparison of *Sl*AacS active site to acetylation substrates and *Sl*AacS homologues

Species	Gene Name/Locus Tag	Accession Number	Percent amino acid identity to *Sl*AacS	Active site motif
S. lividans	*aacS*	ZP_06532271	N/A	610-IPHTLTG**K**RIEVPVK-624
S. lividans	*acs*	ZP_06530204	N/A	603-LPKTRSG**K**IMRRLLR-617
S. enterica	*acs*	NP_463140	N/A	602-LPKTRSG**K**IMRRILR-616
S. enterica	*prpE*	NP_459366	N/A	585-LPKTRSG**K**MLRRTIQ-599
R. palustris	*badA*	NP_946014	N/A	505-LPKTATG**K**IQRFKLR-519
R. palustris	*aliA*	NP_946004	N/A	525-MPATPSG**K**IQKFRLR-539
R. palustris	*prpE*	NP_949838	N/A	591-LPKTRSG**K**ILRGTIK-605
R. palustris	*acs*	NP_945564	N/A	599-LPKTRSG**K**IMRRILR-613
Pseudomonas aeruginosa PAO1	PA1997	NP_250687	46	606-IPRTLSG**K**IVELAVR-620
Archaeoglobus fulgidus	*acs-1*	NP_069035	44	608-IPMTLNY**K**KLEVPIK-622
Caenorhabditis elegans	SUR-5	NP_509229	37	658-IPYTSSG**K**KVEVAVK-672
Rattus norvegicus	AACS	NP_075592	39	370-IPYTING**K**KVEVAVK-384
Homo sapiens	AACS, SUR5	NP_076417	38	626-IPYTLNG**K**KVEVAVK-640